Data Analysis Report

amPD-1 Effects in DIO and WT Mice - Serum Proteomics Results

Client:

Author:

Date:

Contact: info@panomebio.com

Table of Contents

Project Summary

Sample description:

Forty mouse serum samples were received. Twenty of the samples were from DIO mice bearing MC-38 subcutaneous tumors and twenty of the samples were from WT mice with the same tumor model. Ten mice from both the DIO and WT groups were treated with amPD-1 the remaining ten in each group were untreated.

Goal:

To identify and characterize the metabolic differences between the serum of tumor-bearing DIO and WT and to determine the differential metabolic responses to amPD-1 treatment between WT and DIO mice.

Assay summary:

The SomaScan v4.1 assay was performed on 39 of the 40 study samples, one sample from the WT amPD-1 group had insufficient sample volume for analysis.

Analysis summary:

The SomaScan proteomic profiles were normalized and log transformed. Statistical analysis was performed to identify dysregulated proteins between the four sample groups. Proteins showing dysregulation were further analyzed to determine differences in protein abundance as a result of amPD-1 treatment between WT and DIO mice.

Conclusions:

The results of the analysis show diverse proteomic profiles across the sample groups. In particular, there were large differences in protein abundance between DIO and WT mice as well as between DIO treated and untreated mice. Differences between WT treated and untreated mice were relatively minor. Interpretation of these differences revealed that proteins that are involved in the Warburg Effect were elevated in DIO untreated mice relative to WT untreated mice. However, after amPD-1 treatment, the levels of these proteins were reduced. No differences in these proteins were observed after amPD-1 treatment in WT mice.

Experimental Methods

Sample preparation

Sample handling and storage

Serum samples were frozen at -80°C after receipt. Samples were shipped to SomaLogic on dry ice.

SomaScan 4.1 assay

The first step of the SomaScan Assay is the dilution of a biological sample of interest. The sample dilutions are incubated with the respective SOMAmer reagent mixes that have been attached to streptavidin (SA)-coated beads.

The beads are washed to remove non-specifically associated proteins and other matrix constituents. Proteins that remain bound to SOMAmer reagents are tagged using an NHS-biotin reagent. SOMAmer complexes and unbound SOMAmer reagents are released from the SA beads using ultraviolet light that cleaves a photo-cleavable linker within the SOMAmer reagent construct into a solution containing an anionic competitor.

Non-specific interactions dissociate, and the anionic competitor solution prevents them from reforming while specific complexes are maintained. The photo-cleavage eluate, which contains all SOMAmer reagents (some bound to a biotin-labeled protein and some free), is separated from the beads and then incubated with a second streptavidin coated bead that binds the biotin-labeled proteins and the biotin-labeled protein–SOMAmer complexes.

The free SOMAmer reagents are removed during subsequent washing steps. In the final elution step, protein-bound SOMAmer reagents are released

from their proteins using denaturing conditions and recovered. These SOMAmer reagents are then quantified by hybridization to custom DNA microarrays. The cyanine-3 signal from the SOMAmer reagent is detected on microarrays.

Data preprocessing

SomaLogic data standardization

The SomaScan Assay is performed using 96-well plates; eleven wells are allocated for control samples used to control for batch effects and to estimate the accuracy, precision, and buffer background levels of the assay. Five pooled Calibrator Control replicates, three pooled Quality Control (QC) replicates, and three buffer (no protein) replicates are run on each plate.

For core sample types, Calibrator and QC replicates are created by pooling samples of the same type from presumed healthy donors. Twelve Hybridization Control SOMAmer reagents not exposed to sample proteins are added during the SOMAmer reagent elution step to control for readout variability.

The control samples are run repeatedly during assay qualification and robust point estimates are generated and stored as references for each SOMAmer reagent result for the Calibrator and QC samples. The results are to be used as references throughout the life of the SomaScan Assay version.

Raw SomaScan Assay data may contain systematic biases from many sources, such as technical variation introduced by the readout, pipetting errors, or consumable reagent changes; more significantly, pre-analytical variance related to sample collection methods or inherent sample variation in overall protein levels leads to additional nuisance variance. Data standardization procedures are used to

mitigate technical variation.

Data standardization is comprised of normalization and calibration which are routine numerical procedures developed to remove systematic biases in raw assay data after microarray feature aggregation.

In general, normalization is a sample-by-sample adjustment to overall signals within dilution bins (plasma and serum) or signaling bins (urine). Calibration is an overall plate adjustment and a SOMAmer-by-SOMAmer adjustment that decreases between-plate variability.

Each normalization method computes a scale factor, or set of scale factors, for each sample or SOMAmer reagent that is subsequently applied to the signal.

The data standardization steps include the following:
1. Hybridization normalization
2. Intra plate signal normalization of Calibrator and Buffer (no protein) replicates
3. Plate scale standardization and Calibration using a global calibrator reference
4. Signal normalization of the QC replicates using a global signal normalization reference
5. QC check of the median of QC replicate values to the global QC reference standard specific for the pooled QC lot on the plate
6. Signal normalization of the individual samples using a global signal normalization reference

All individual, QC, and Buffer samples are then median normalized to a reference value. Median Normalization to a Reference can be performed on a single sample due to the presence of an external global reference value generated from a cohort of healthy normal individuals for each SOMAmer reagent for our core matrices. A ratio is computed for each SOMAmer reagent by dividing the global reference SOMAmer RFU by its measured RFU in the sample to be normalized. The median of the SOMAmer measurement ratios for all SOMAmer reagents in a dilution defines the sample-based scale factor for all SOMAmer reagents within that dilution and sample. All SOMAmer reagents within the dilution for a sample are scaled by the resulting median signal scale factor. Three sample dilutions will result in three independent median signal scale factors for each sample in addition to the hybridization scale factor. We then iterate this approach up to 100 times until convergence occurs. Only ratios within 2 standard deviations of the mean will be considered for calculating scale factors. This approach is known as Adaptive Normalization by Maximum Likelihood, or ANML. If the samples are a non-core matrix, we assemble an intra-study reference via bootstrapping and calculate the ratios from that reference to individual samples. After normalization, the relative protein abundances are written to the SomaLogic .adat file format.

Relative protein abundances after Adaptive ANML were extracted from the SomaLogic .adat files. Proteins missing NCBI gene or UniProt identifiers were removed as these represent control proteins. Duplicate protein signals (from multiple SomaMers) were removed and replaced with the mean signal across all SomaMers for the protein. Relative protein abundances were then log10 transformed prior to statistical analysis.

Statistical analysis

Hypothesis testing was performed with a two-tailed, two-sample t-test with unequal variance. Log2 transformed protein abundances were used for null hypothesis testing. The resulting p-values were corrected with the Benjamini-Hochberg Procedure. Fold-changes were computed from non-log2 transformed values.

Over-representation analysis was performed with a Fisher's Exact test that compares the expected number of proteins found to be statistically significant in each pathway with the number of significant proteins found in each pathway. For null hypothesis testing, a corrected p-value cutoff of 0.05 and an absolute log2 fold change of 1.0 was used. For the over-representation analysis, only the p-value cutoff was used.

Results

Protein associations

After filtration, relative abundance values for 6,418 proteins were available for analysis. The relative abundances of these proteins form the proteomic profiles of the samples. The global trends in the proteomic profiles of the serum and liver samples are visualized below in the principal components analysis (PCA, Figure 1) and heatmap (Figure 2) below. Untreated WT samples are shown in blue, treated WT samples are shown in green, untreated DIO samples are shown in purple, and treated DIO samples are shown in red. When considering all proteins, there is no visible clustering by sample group.
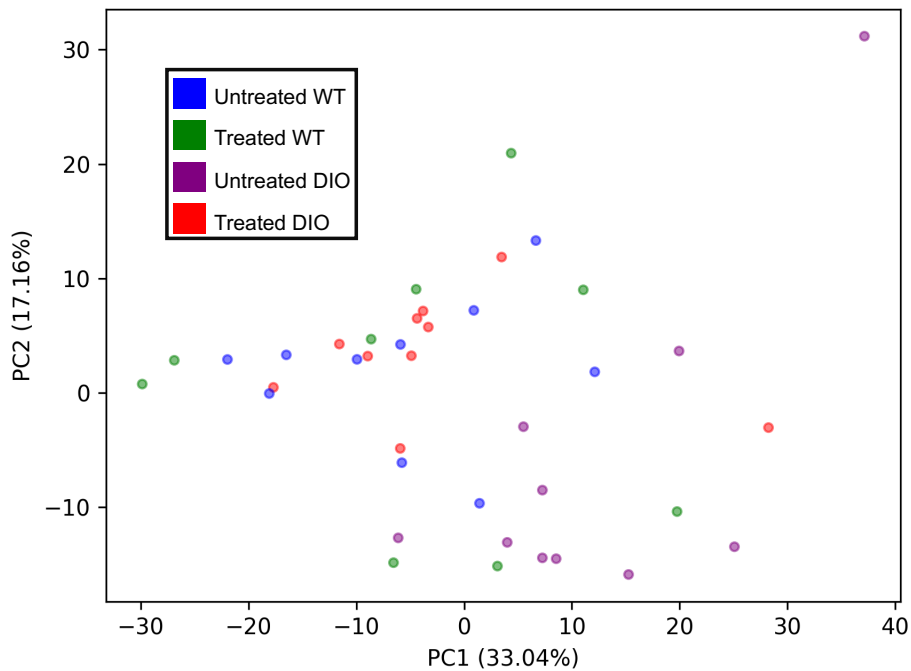
Figure 1: Principal components analysis of serum proteomics data. The proteomic profiles for each sample are visualized in the scatter plot above. Each dot represents a sample. Untreated WT samples are shown in blue, treated WT samples are shown in green, untreated DIO samples are shown in purple, and treated DIO samples are shown in red.
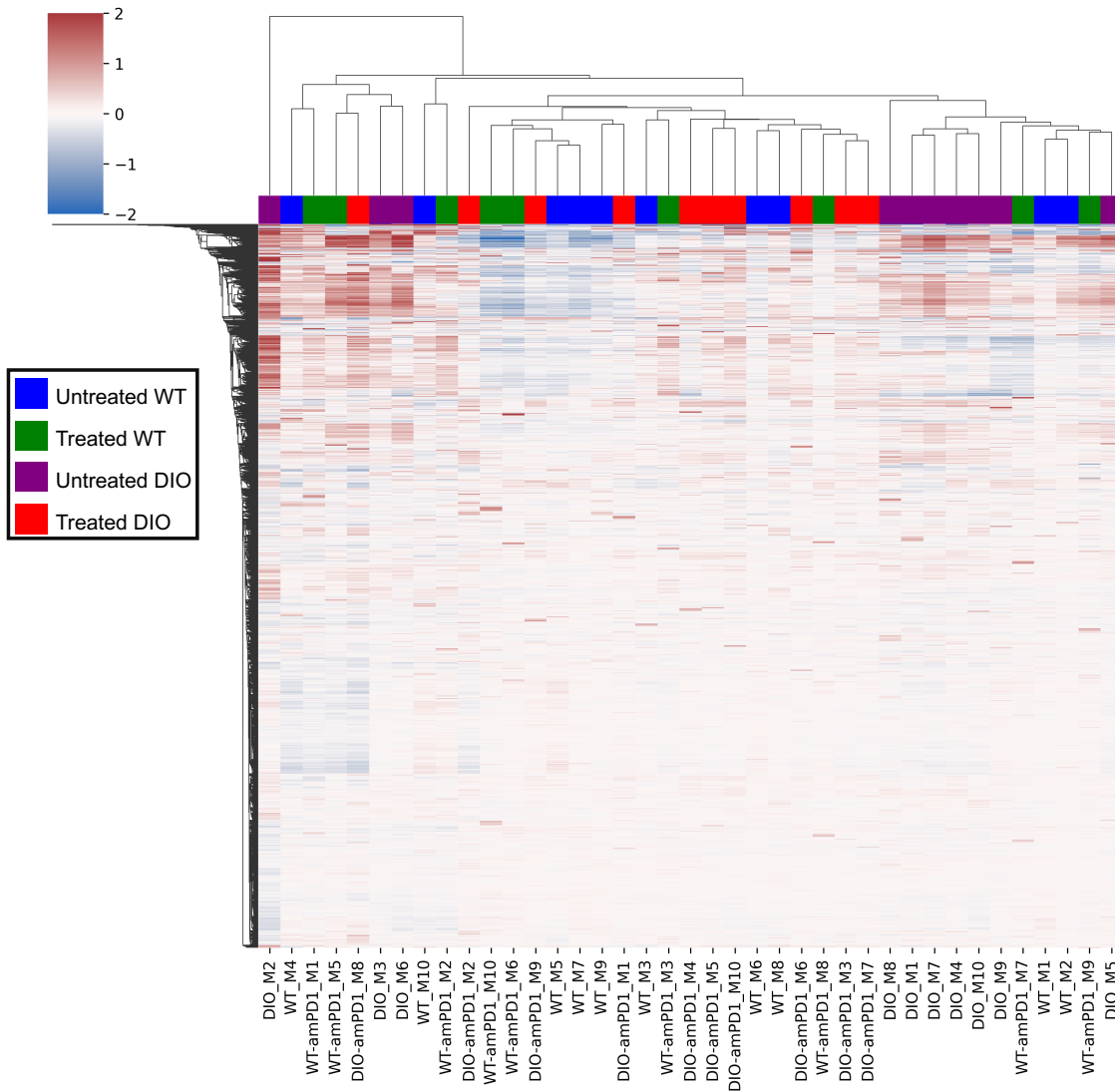
Figure 2: Heatmap of serum proteomics data. The proteomic profiles for each sample are visualized in the heatmap above. Each column represents a sample, and each row represents a protein. Columns are colored according to experimental group. Untreated WT samples are shown in blue, treated WT samples are shown in green, untreated DIO samples are shown in purple, and treated DIO samples are shown in red. The color of each cell indicates the log2(fc) relative to the mean untreated WT level of each protein.

To determine what proteins have altered abundance across the four sample groups, null hypothesis testing was performed on all profiled proteins, revealing 673 significantly altered proteins (having a corrected p-value (q) of less than 0.05) between at least two of the sample groups. When considering only these 673 proteins, we now see clustering by sample group in the PCA (Figure 3) and heatmap (Figure 4). Only the top fifty most significant proteins are shown in Figure 4. The largest alterations are between DIO and WT samples, with the majority of alterations resulting in increased protein abundance in DIO samples relative to WT samples. Additionally, we see decreases in the abundance of many proteins after amPD-1 treatment in DIO mice.
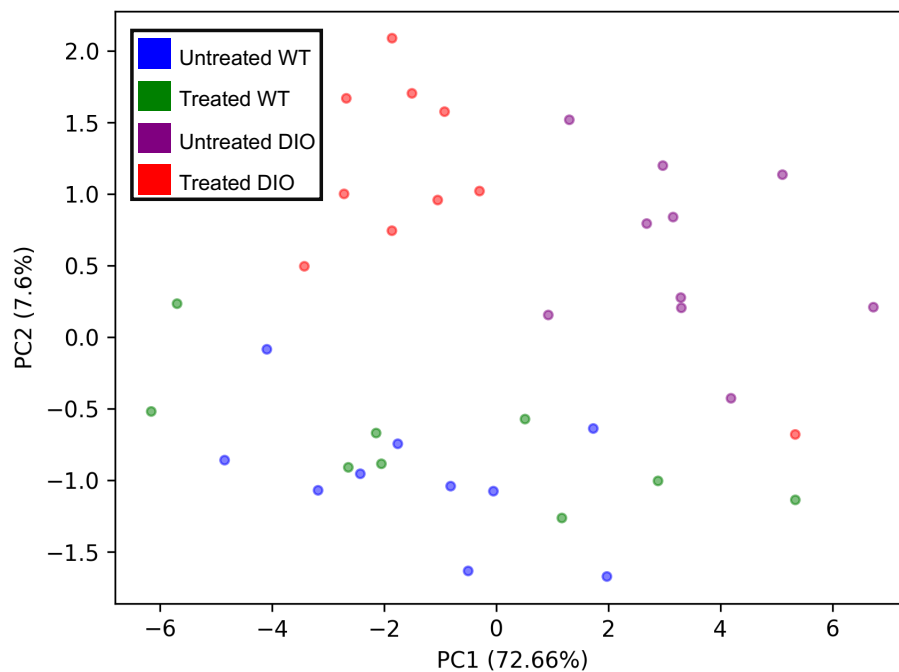
Figure 3: Principal components analysis of serum proteomics data considering only significantly altered proteins. The proteomic profiles composed of only the statistically significant proteins for each sample are visualized in the scatter plot above. Each dot represents a sample. Untreated WT samples are shown in blue, treated WT samples are shown in green, untreated DIO samples are shown in purple, and treated DIO samples are shown in red.
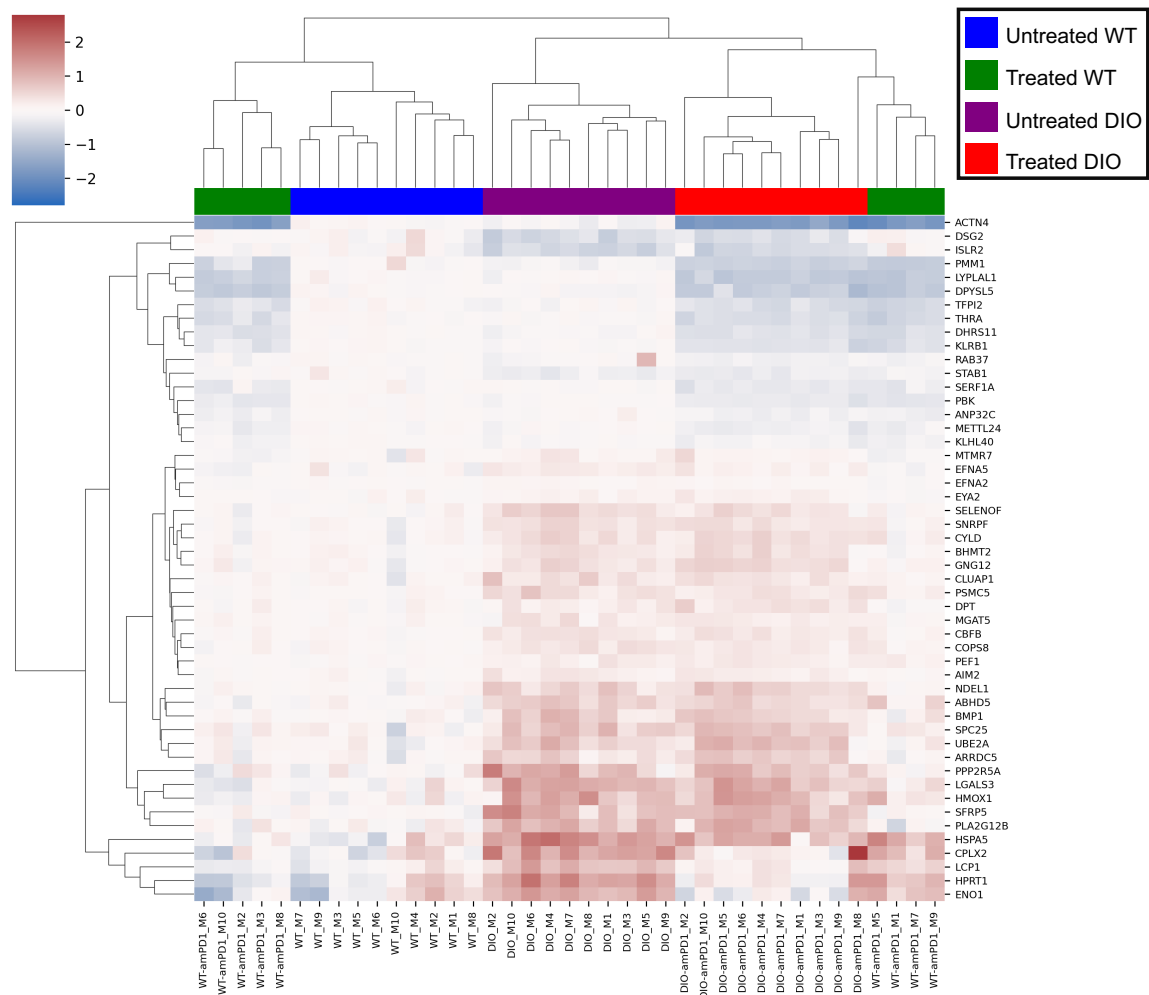
Figure 4: Heatmap of significantly altered serum proteins. The log2(fc) of protein abundances relative to the WT untreated serum samples is shown in the heatmap for the top 50 most significantly altered proteins between the four sample groups. Each column represents a sample, and each row represents a protein. Columns are colored according to experimental group. Untreated WT samples are shown in blue, treated WT samples are shown in green, untreated DIO samples are shown in purple, and treated DIO samples are shown in red.

To determine specific biological alternations coming from amPD-1 treatment, null hypothesis testing between both treated and untreated WT and DIO samples was performed on the 673 proteins elucidated in the previous analysis. In total, 430 of these proteins had a statistically significant difference (p-value < 0.05) between treated and untreated samples in at least one sample type (DIO or WT mice). The DIO mice showed an overall stronger response to amPD-1 treatment with the majority of these proteins only showing a response in DIO mice (Figure 5).
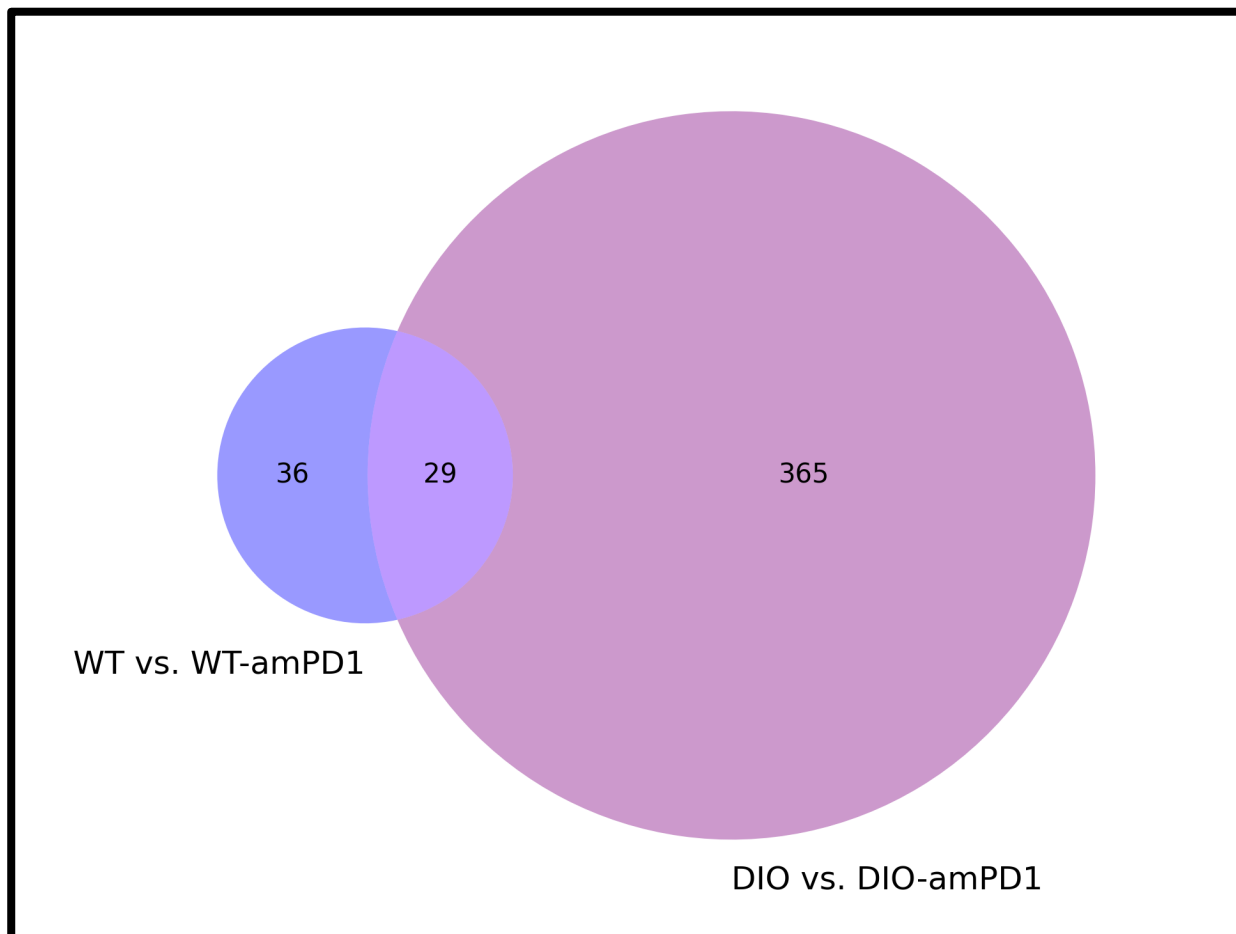
Figure 5: Venn diagram of treatment effects in DIO and WT mice. The significant protein alterations between treated and untreated DIO and WT mice are compared in the Venn diagram above. The WT and DIO mice show little similarity in the proteomic signature of treatment.

To visualize the protein alterations after amPD-1 treatment in WT and DIO mice, heatmaps showing the statistically significant protein alterations shared between both DIO and WT mice, unique to WT mice, and unique to DIO mice are provided in Figure 6, Figure 7, and Figure 8, respectively.
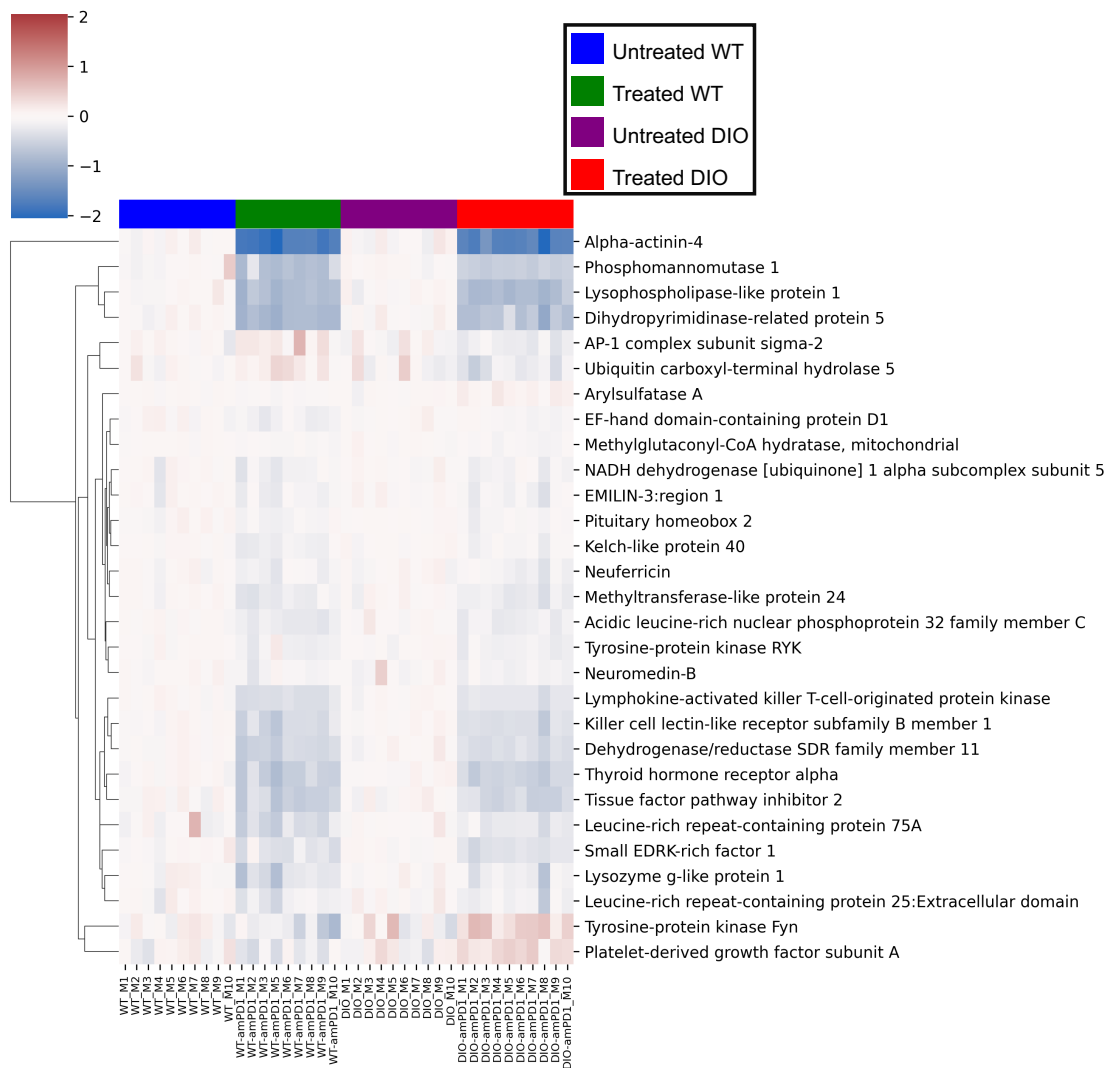
Figure 6: Heatmap of proteins altered with amPD-1 treatment in both WT and DIO mice. The log2 fold-changes (relative to the mean abundance in the untreated WT samples) of the proteins significantly altered (p-value < 0.05) between DIO treated vs. untreated and WT treated vs. untreated are plotted for each experimental group. Columns are colored according to experimental group. Untreated WT samples are shown in blue, treated WT samples are shown in green, untreated DIO samples are shown in purple, and treated DIO samples are shown in red.
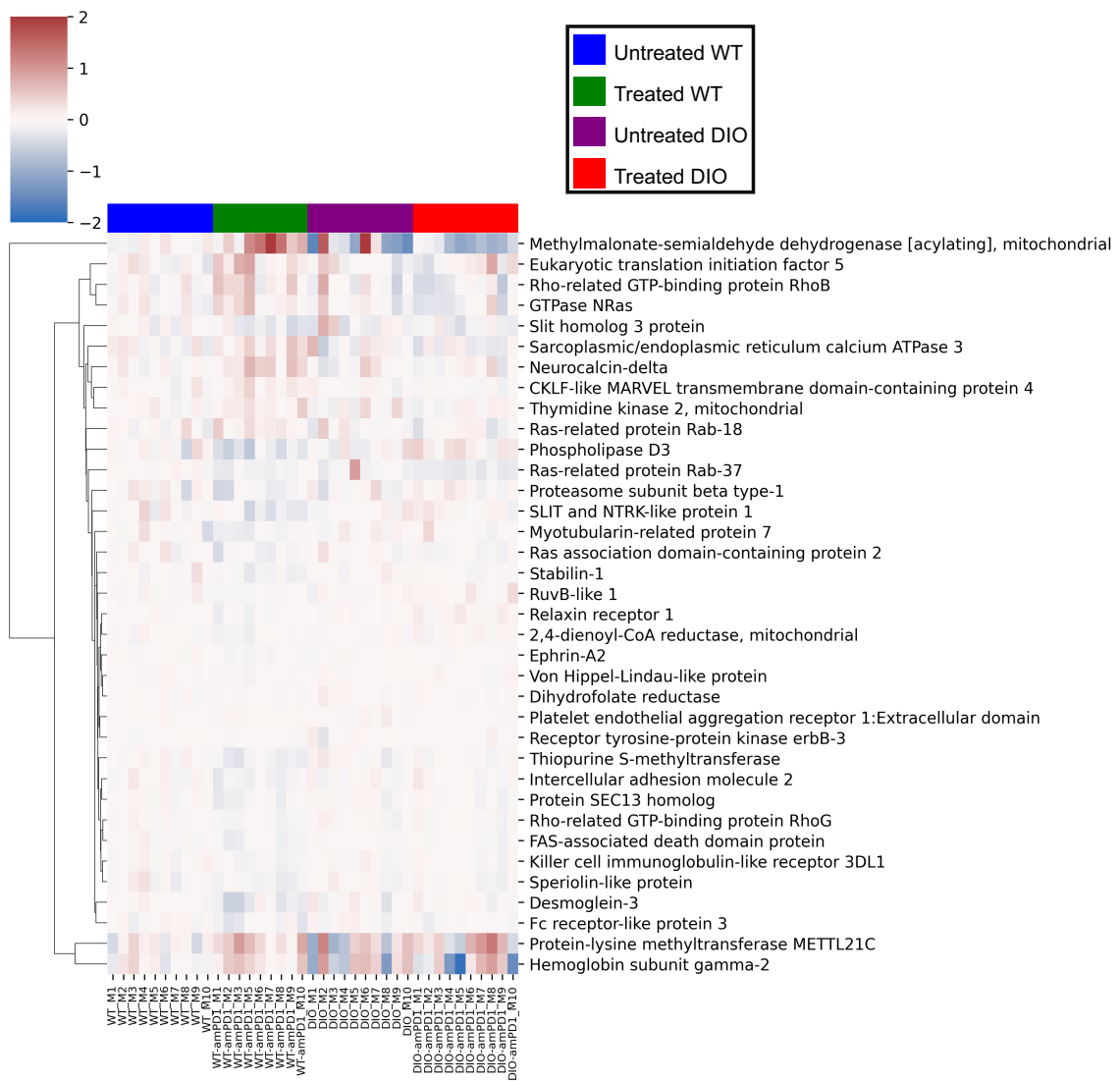
Figure 7: Heatmap of proteins altered with amPD-1 treatment in only WT mice. The log2 fold-changes (relative to the mean abundance in the untreated WT samples) of the proteins significantly altered (p-value < 0.05) between WT treated vs. untreated samples but not between DIO treated and untreated samples are plotted for each experimental group. Columns are colored according to experimental group. Untreated WT samples are shown in blue, treated WT samples are shown in green, untreated DIO samples are shown in purple, and treated DIO samples are shown in red.
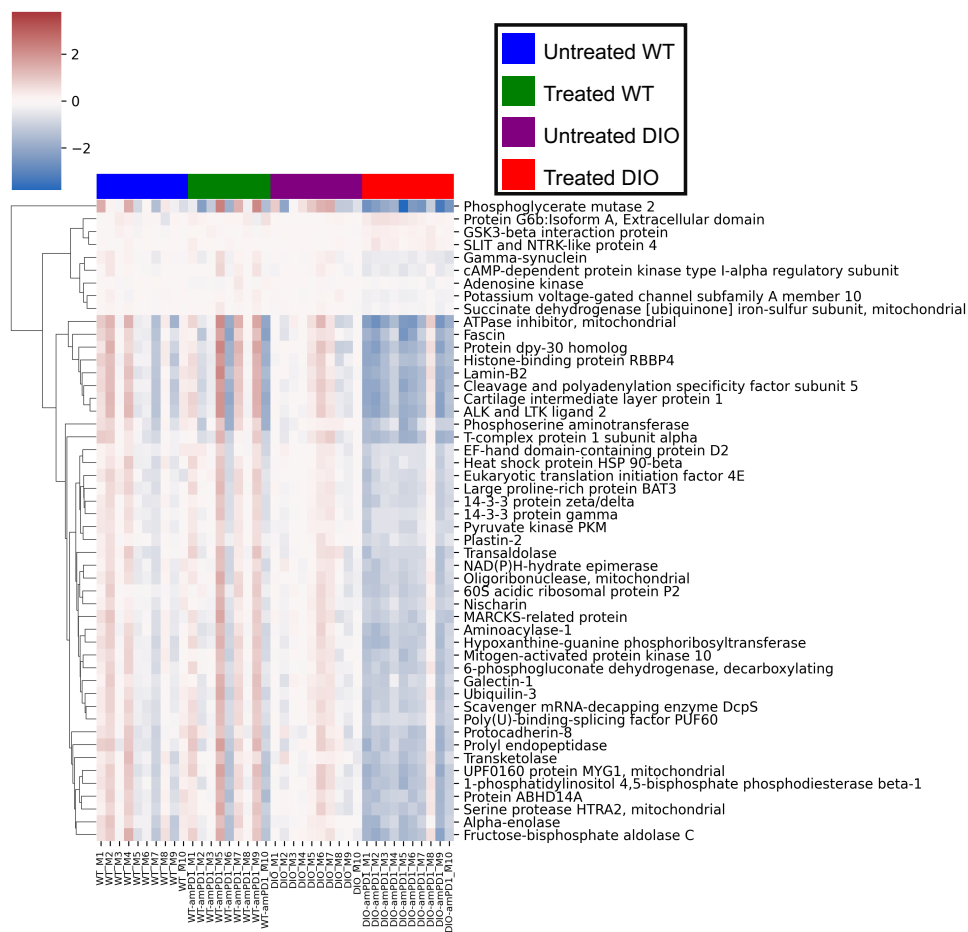
Figure 8: Heatmap of top 50 proteins altered with amPD-1 treatment in only DIO mice. The log2 fold-changes (relative to the mean abundance in the untreated WT samples) of the proteins significantly altered (p-value < 0.05) between DIO treated vs. untreated but not between WT treated vs. untreated are plotted for each experimental group. Columns are colored according to experimental group. Untreated WT samples are shown in blue, treated WT samples are shown in green, untreated DIO samples are shown in purple, and treated DIO samples are shown in red.

Interpretation

To gain biological insight into the protein alterations detected across all four sample groups, we first performed an over-representation analysis on the 592 proteins with statistically significant changes in abundance between untreated DIO and WT mice (Figure 9). The analysis revealed two pathway alterations, the most significantly being the Warburg Effect, a hallmark of cancer metabolism. A closely related pathway, glycolysis, was also enriched.
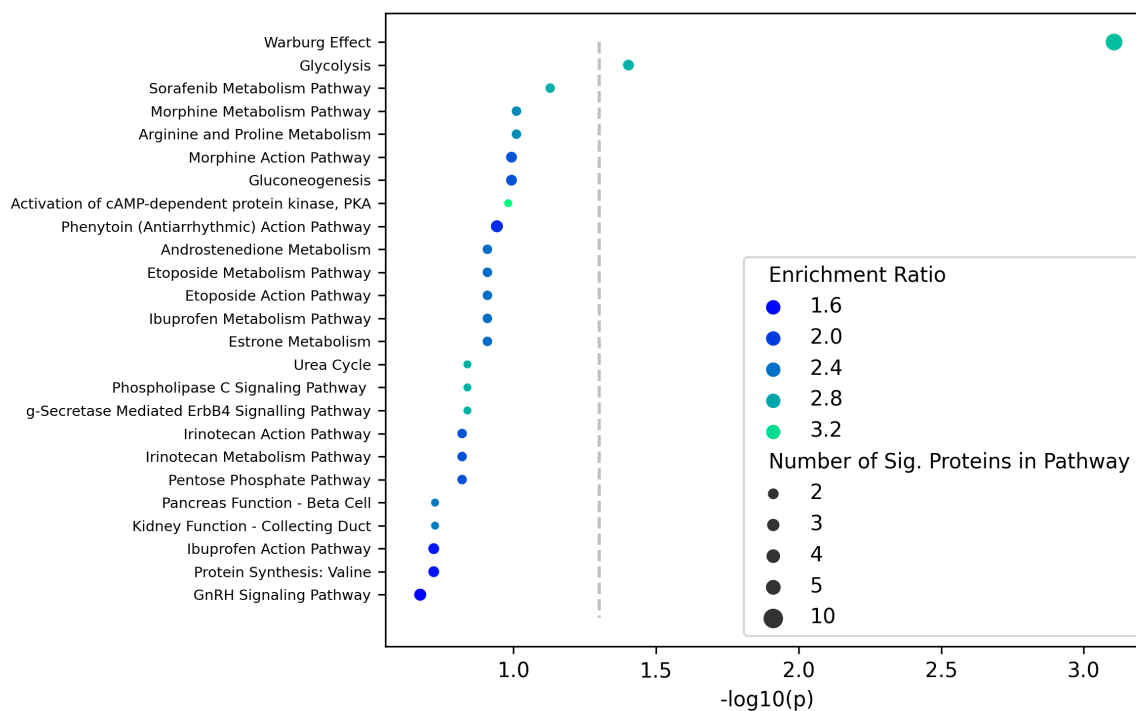
Figure 9: Pathway analysis of significant proteins alterations between untreated DIO and WT mice. The pathways found to be enriched between untreated WT and DIO mice are shown in the dot plot with their corresponding significance levels on the x-axis. The grey dashed line indicates the p = 0.05 significance threshold. The size of the dots indicates the number of proteins that were statistically different between the sample groups, and the color indicates the enrichment ratio (the number of statistically significant proteins observed in the pathway divided by what is expected by random chance).

Next, to interpret the differences in response of amPD-1 treatment, we again performed pathway analysis on the protein alterations present after amPD-1 treatment in WT mice (Figure 10) and DIO mice (Figure 11). Notably, there was no overlap between the enriched pathways found in DIO and WT mice.
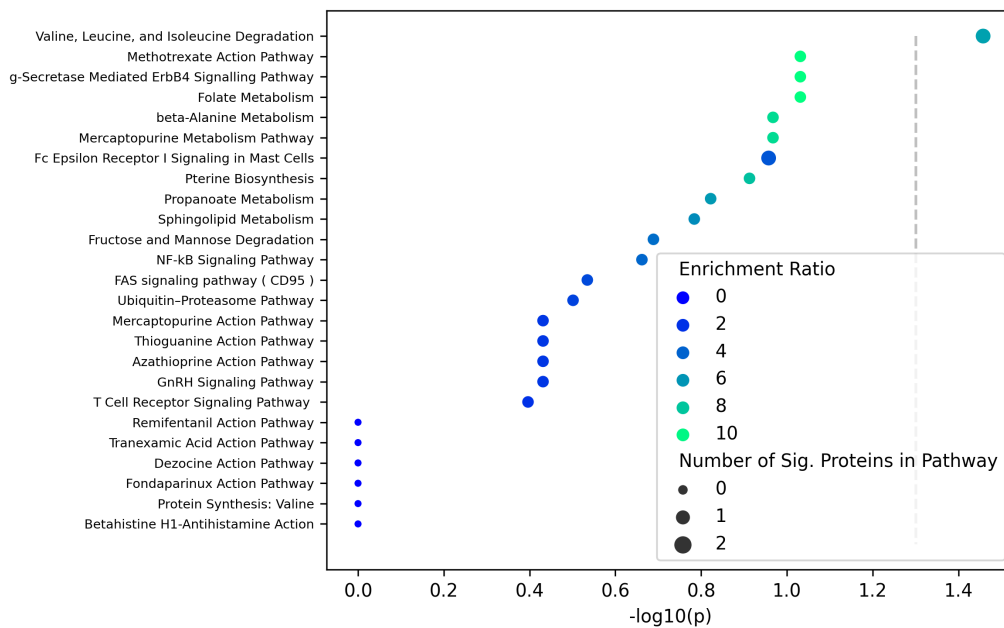
Figure 10: Pathway analysis of significant proteins alterations between untreated and treated WT mice.
The pathways found to be enriched between untreated WT and treated WT mice are shown in the dot plot with their corresponding significance levels on the x-axis. The grey dashed line indicates the p = 0.05 significance threshold. The size of the dots indicates the number of proteins that were statistically different between the sample groups, and the color indicates the enrichment ratio (the number of statistically significant proteins observed in the pathway divided by what is expected by random chance).
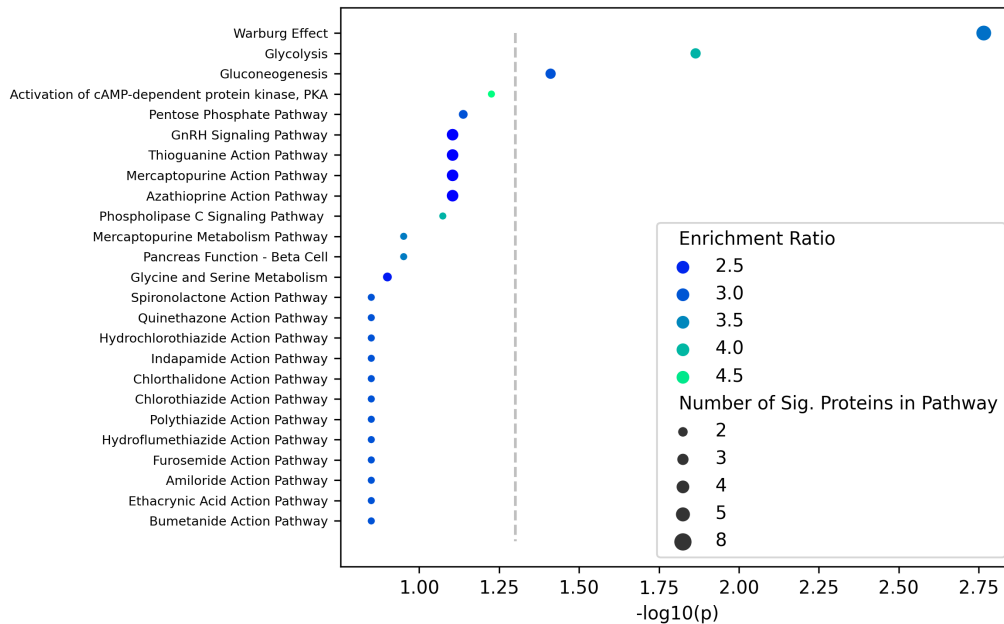
Figure 11: Pathway analysis of significant proteins alterations between untreated and treated DIO mice.
The pathways found to be enriched between untreated DIO and treated DIO mice are shown in the dot plot with their corresponding significance levels on the x-axis. The grey dashed line indicates the p = 0.05 significance threshold. The size of the dots indicates the number of proteins that were statistically different between the sample groups, and the color indicates the enrichment ratio (the number of statistically significant proteins observed in the pathway divided by what is expected by random chance).

In WT mice, amPD-1 treatment resulted in enrichment of one pathway: valine, leucine, and isoleucine degradation. Two metabolites in this pathway were enriched, methylmalonate-semialdehyde dehydrogenase (Figure 12a) and methylglutaconyl-CoA hydratase (Figure 12b). Interestingly, methylmalonate-semialdehyde dehydrogenase abundance is only altered after treatment in WT mice.
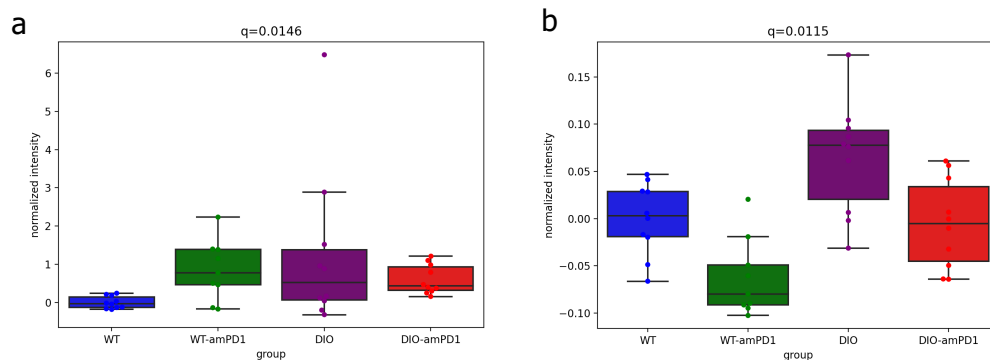
Figure 12: Significantly altered valine, leucine, and isoleucine degradation proteins. The log2(fc) of protein abundances relative to the WT untreated serum samples is shown in the boxplots. In (a), the fold changes for methylmalonate-semialdehyde dehydrogenase is shown. In (b), the fold changes for methylglutaconyl-CoA hydratase is shown.

In DIO mice, three pathways were enriched: the Warburg effect, glycolysis, and gluconeogenesis. However, the proteins that drive the enrichment of glycolysis and gluconeogenesis were a subset of the dysregulated Warburg effect proteins. Of the 29 Warburg effect proteins measured in the experiment, 10 were significantly altered between DIO treated and untreated samples. The abundance of the dysregulated Warburg effect proteins across all samples is shown in Figure 13. Among these proteins, the largest change in abundance was in phosphoglycerate mutase 2, which interconverts 3-phosphoglycerate and 2-phosphoglycerate in glycolysis and gluconeogenesis (Figure 14). Additionally, many of the Warburg effect proteins also participate in the oxidative and non-oxidative phases of the pentose phosphate pathway (PPP), such as 6-phosphogluconate dehydrogenase (oxidative PPP, Figure 15a) and transketolase (non-oxidative PPP, Figure 15b). Notably, both of these proteins were higher in untreated DIO mice relative to WT untreated mice. After treatment, levels in DIO mice are reduced to WT levels, while treatment in WT caused no change in the abundance of these proteins.
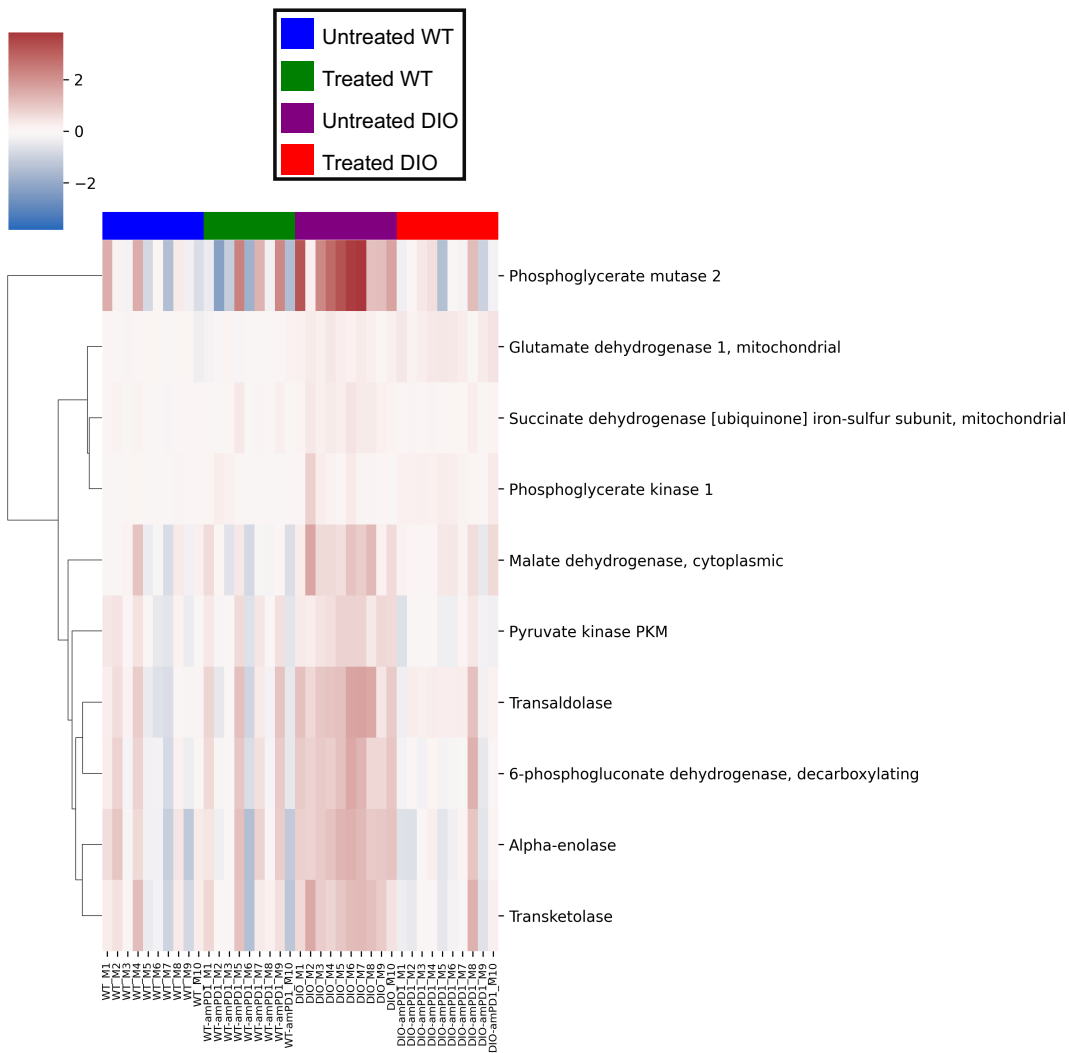
Figure 13: Heatmap of significantly altered Warburg effect proteins. The log2(fc) of protein abundances relative to the WT untreated serum samples is shown in the heatmap for the significantly altered proteins that participate in the Warburg Effect pathway. Each column represents a sample, and each row represents a protein. Columns are colored according to experimental group. Untreated WT samples are shown in blue, treated WT samples are shown in green, untreated DIO samples are shown in purple, and treated DIO samples are shown in red.
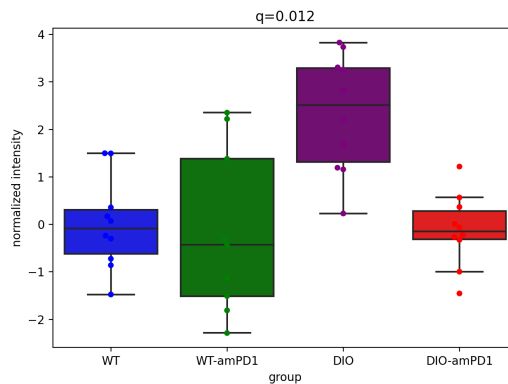
Figure 14: Dysregulation in phosphoglycerate mutase 2. The log2(fc) of protein abundance relative to the WT untreated serum samples is shown in the boxplots.
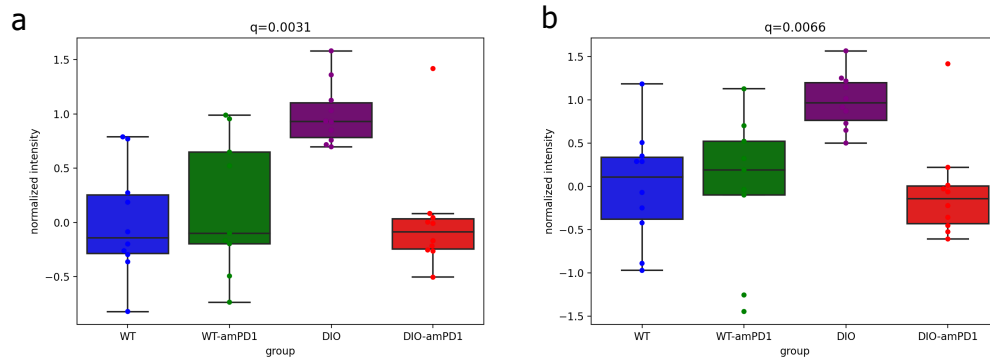
Figure 15: Significantly altered pentose phosphate pathway proteins. The log2(fc) of protein abundances relative to the WT untreated serum samples is shown in the boxplots. In (a), the relative abundance for 6-phosphogluconate dehydrogenase is shown. In (b), the relative abundance for transketolase is shown.

Appendix

Supplementary Files

1. raw_data.zip: .adat files, summary of quality control analysis, and description of SomaScan normalization procedures.

2. SupplementaryTables.xlxs: excel file containing sample metadata, protein information, protein abundances, and the detailed results of the statistical analyses.

3. Plots.zip: high-resolution images for all figures in this report as well as boxplots showing the abundance of each protein across all experimental conditions.